Supporting Information for

Interfacial Self-assembled GR/GO Ultrathin Membranes in Large Scale for Molecular Sieving

Junyuan Xia,[ab] Peng Xiao,[a] Jincui Gu,*[ab] Tianyu Chen,[a] Chaohui Liu,[c] Luke Yan,*[c] Tao Chen*[abc]

[a] Key Laboratory of Marine Materials and Related Technologies, Zhejiang Key Laboratory of Marine Materials and Protective Technologies, Ningbo Institute of Material Technology and Engineering, Chinese Academy of Science, Ningbo 315201, China.

[b] University of Chinese Academy of Science, Beijing 100049, China.

[c] Polymer Materials & Engineering Department, School of Materials Science & Engineering, Chang' an University, Xi'an 710064, China.

E-mail: gujincui@nimte.ac.cn, yanlk_79@hotmail.com, tao.chen@nimte.ac.cn.

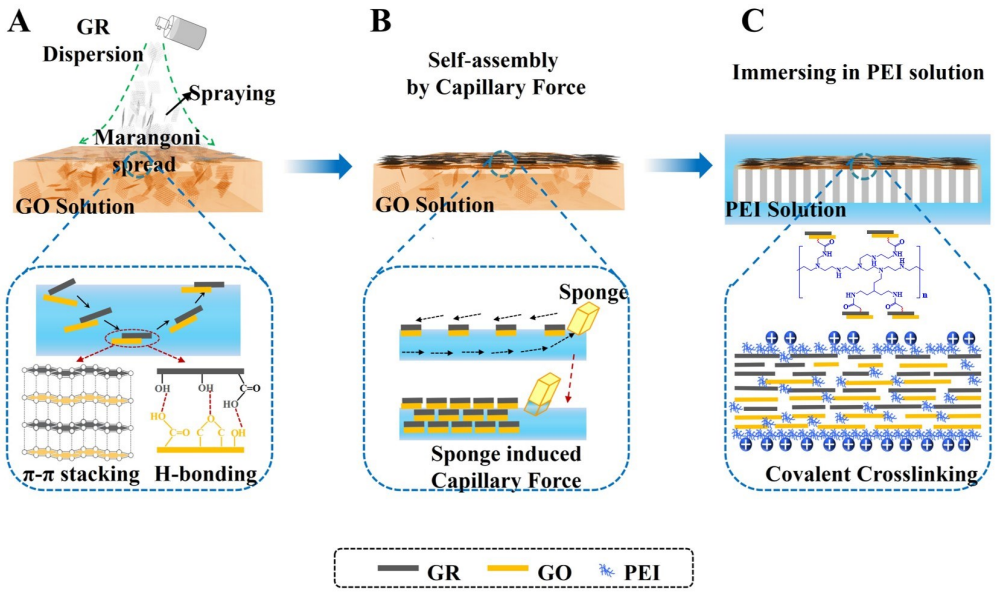

Fig. S1 Schematic illustration of the construction of the GR/GO@PEI composite membrane through the self-assembly process at air/water interface. (A) GR ethanol dispersion was evenly spayed onto the air/GO dispersion interface. In this process, the π-π stacking and the hydrogen bond force between GR and GO promoted the formation of GR/GO layer at the water surface. (B) A porous sponge was applied to compress the GR/GO membrane from a loosely mode to a closely packed state on the air/water surface. (C) The GR/GO membrane was immersed in PEI solution. In this process, PEI was served as a molecular bridge through forming a strong covalent bond with the GR/GO nanosheets.

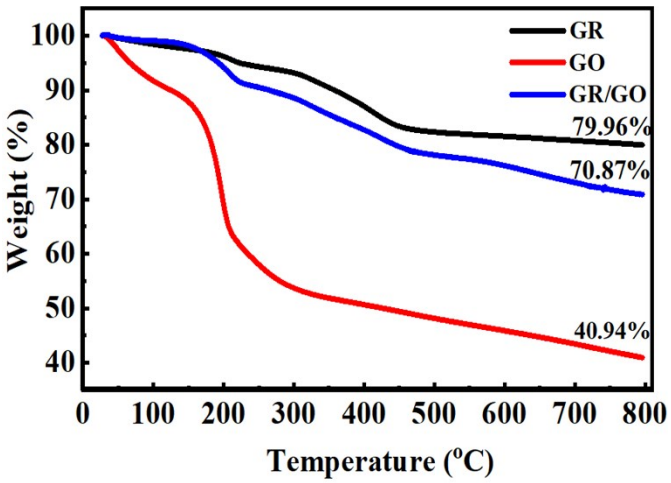

Fig. S2 TGA results of the GO, GR and the GR/GO membrane, respectively.

In order to obtain the ratio of GR and GO in the GR/GO membrane, we need to peel off the GR membrane and GR/GO membrane from the PVDF substrate, respectively. Unfortunately, it was extremely difficult to obtain a whole GR membrane and GR/GO membrane without substance due to their ultrathin thickness. Therefore, it was difficult for us to get the precise proportion form current characterization methods. In spite of this, TGA were also used to assess the approximate relative mass ratio of the GR and GO in the GR/GO membrane. As shown in **Fig. S2,** the weight loss of the pristine purified GR and GO at 800 °C under nitrogen were 79.96 % and 40.94 %, respectively. With respect to the GR/GO membrane, the weight loss was about 70.87%. Therefore, it can be deduced that the mass ratio of the GR and GO was about 3:1.

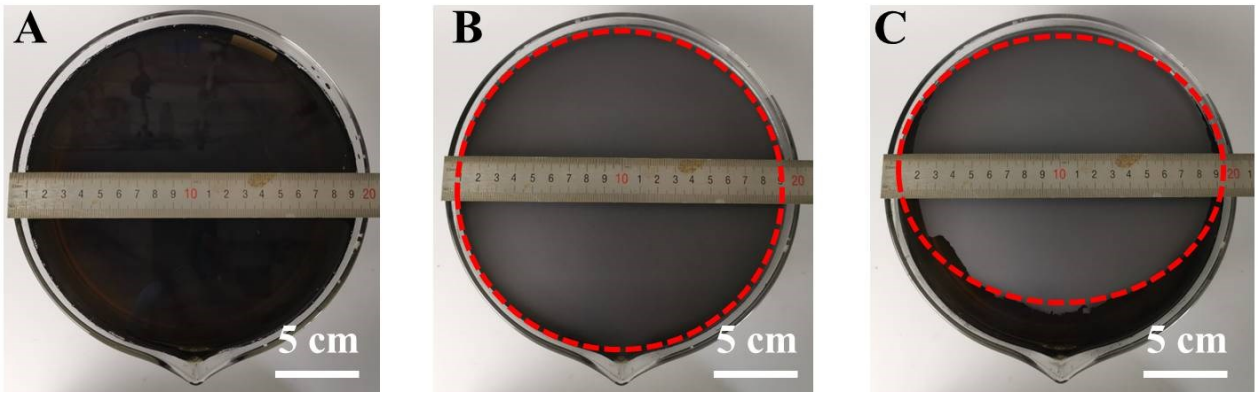

Fig. S3 Self-assembly process of the GR/GO membrane at the air/water interface.

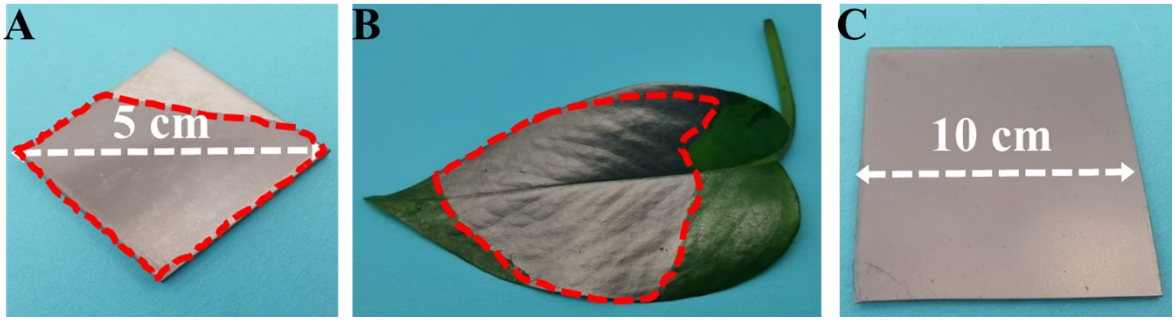

Fig. S4 The free-standing GR/GO membrane can be transferred to any given substance, (A) polystyrene, (B) leaves, (C) silicon.

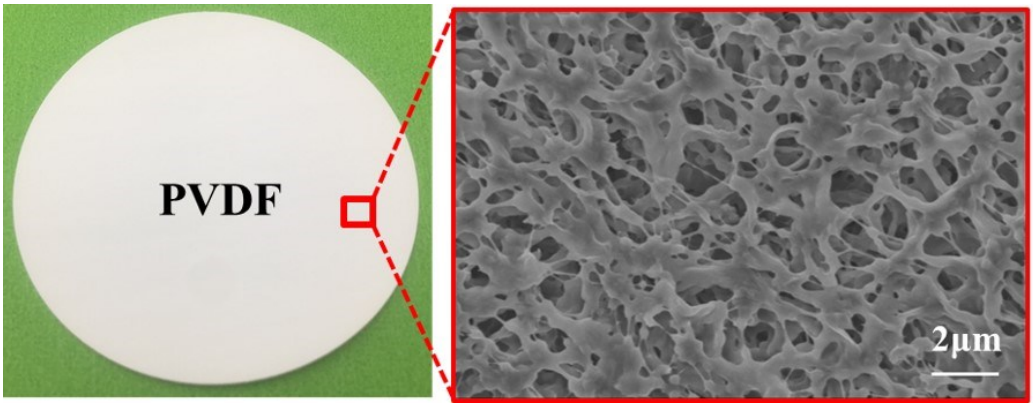

Fig. S5 Photograph of the PVDF substance membrane and its SEM image.

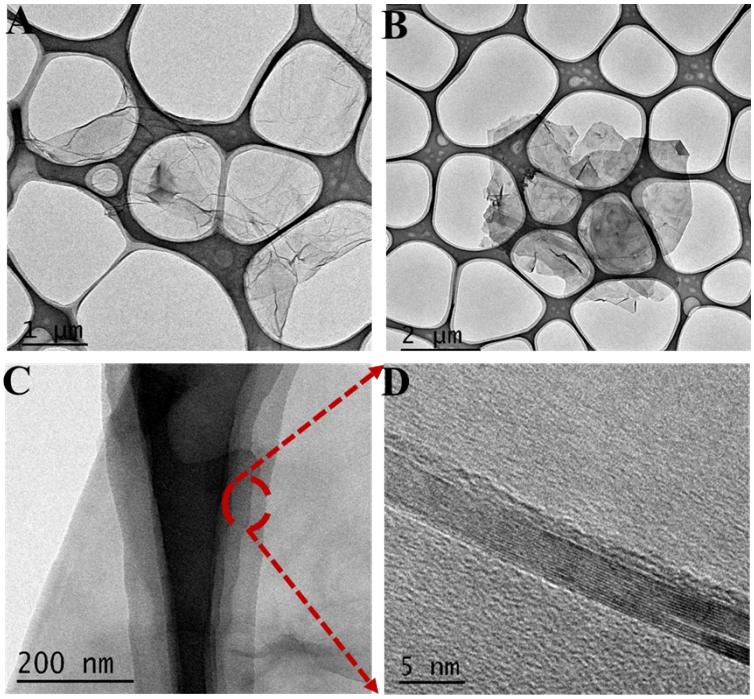

Fig. S6 TEM images of the GO (A), GR (B-C) and the cross-section of GR (D).

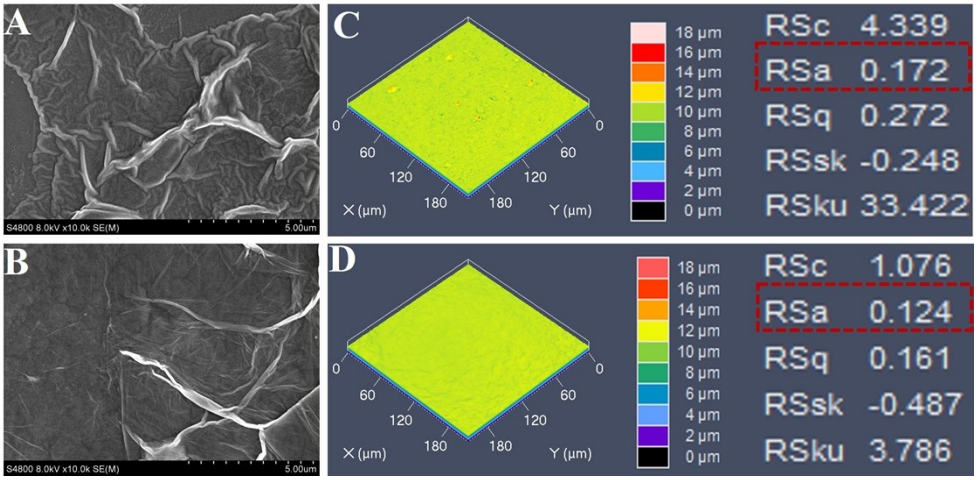

Fig. S7 SEM images of the (A) GR membrane and (B) GO membrane. The laser scanning confocal microscope image of the (C) GR membrane and (D) GO membrane and there responding roughness.

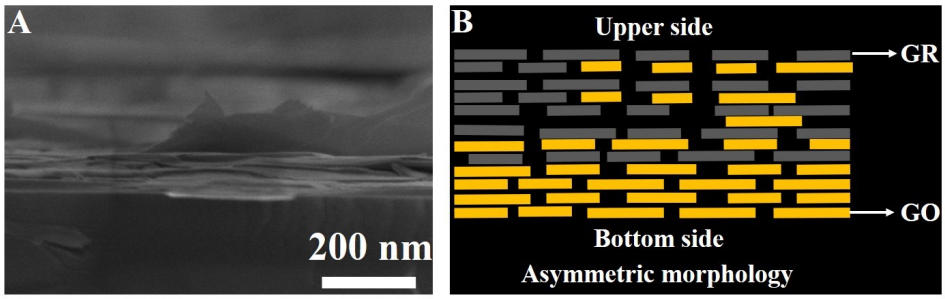

Fig. S8 (A) The cross-sectional SEM image of the GR/GO membrane. (B) The schematic of the structure of the GR/GO membrane.

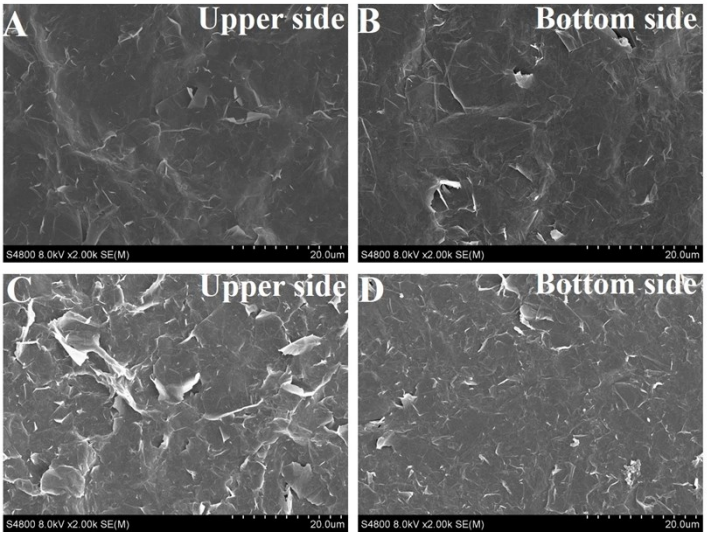

Fig. S9 SEM images of the upper side (A, C) and the bottom side (B, D) of the GR/GO membrane and GR/GO@PEI composite membrane, respectively.

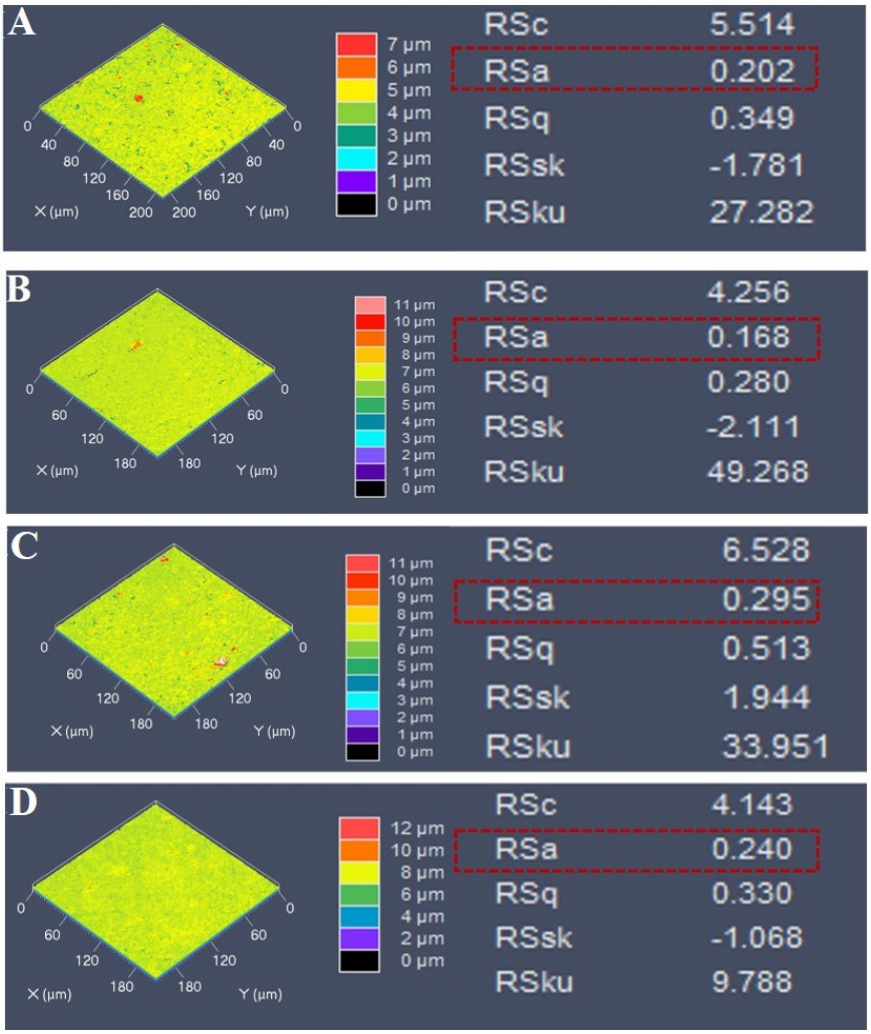

Fig. S10 The laser scanning confocal microscope image of the (A, C) upper and (B, D) bottom sides of the GR/GO membrane and GR/GO@PEI composite membrane and their responding roughness.

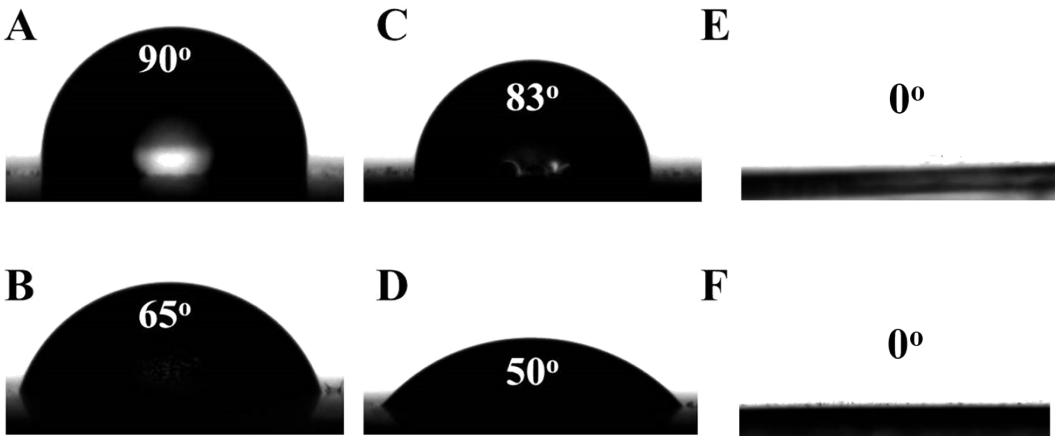

Fig. S11 Wettability of the upper side (A, C, E) and the bottom side (B, D, F) of the GR membrane, the GR/GO membrane and the GR/GO@PEI composite membrane, respectively.

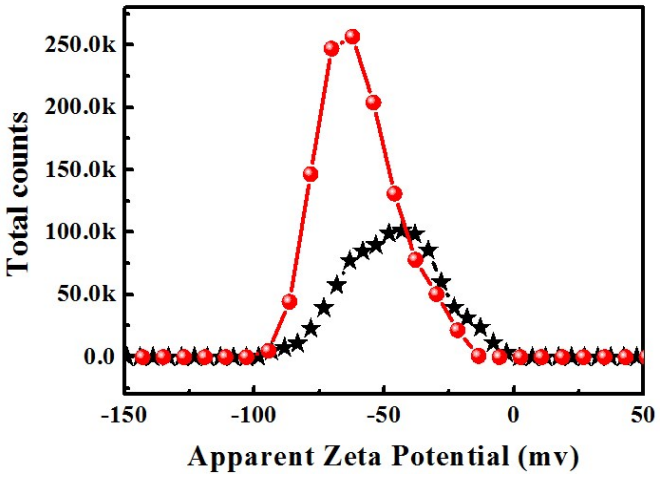

Fig. S12 The zeta potential of the GO (black) solution and GR/GO (red) solution.

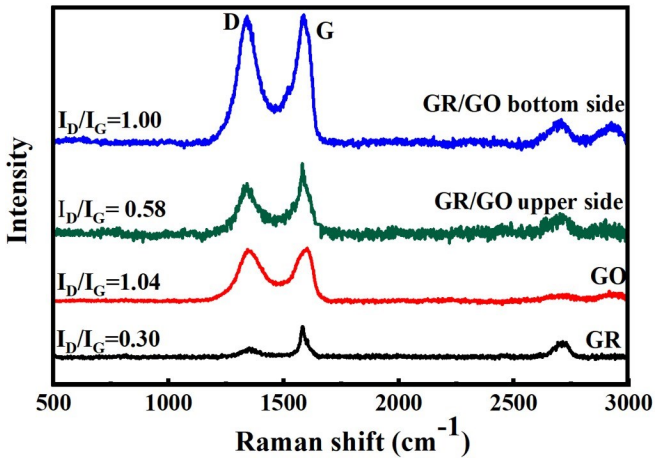

Fig. S13 Raman spectra of the GO membrane, GR membrane, and the both sides of the GR/GO membrane, respectively.

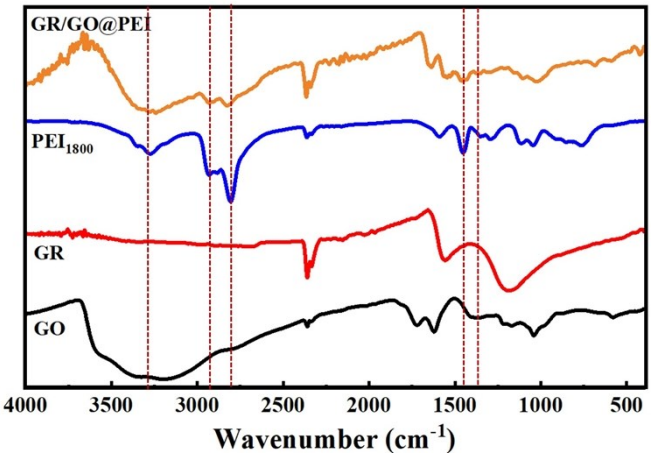

Fig. S14 IR spectra of the GO, GR, PEI_{1800} and GR/GO@PEI_{1800}.

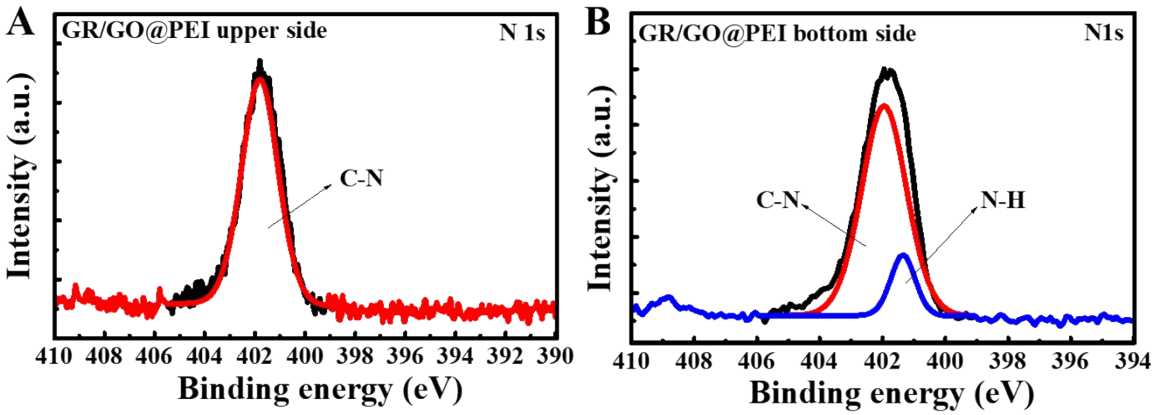

Fig. S15 N1s spectrum of the upper (A) and the bottom side (B) of the GR/GO@PEI composite membrane, respectively.

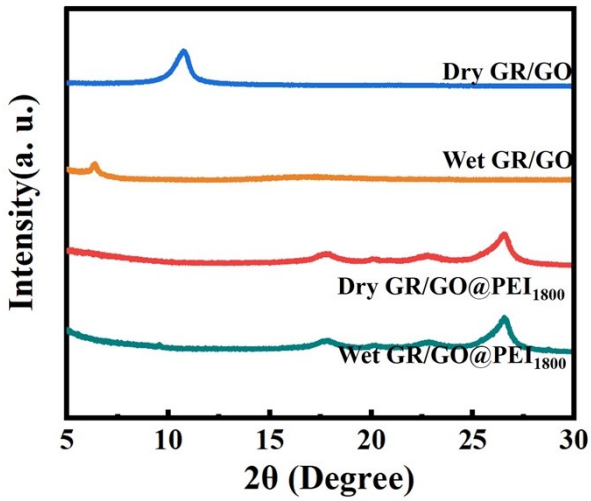

Fig. S16 XRD patterns of the GR/GO membrane and the GR/GO@PEI composite membrane in dry and wet states, respectively.

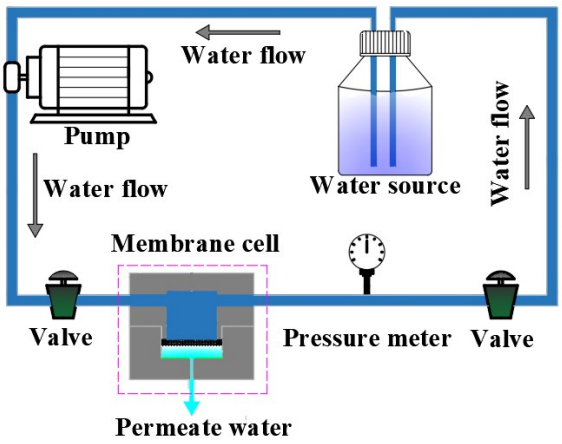

Fig. S17 The schematic illustration of the homemade cross-flow filtration apparatus.

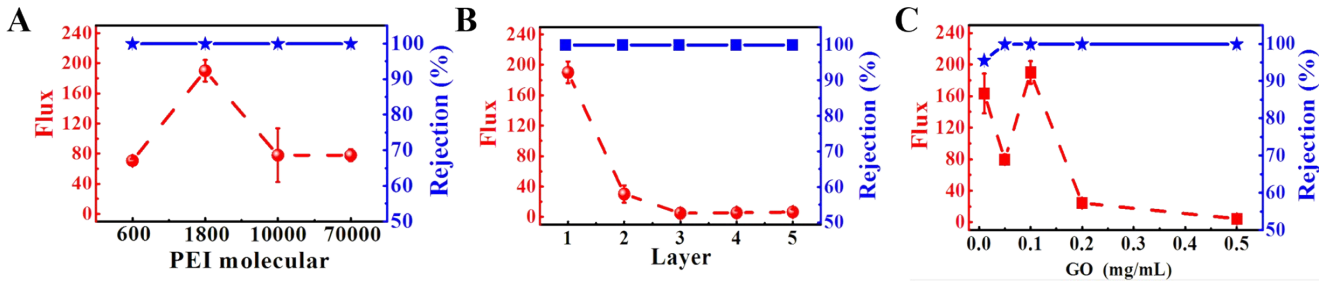

Fig. S18 The effect of molecular weight of PEI (A), different GR/GO layer (B) and the concentration of GR (C) on the separation flux and efficiency of GR/GO@PEI_{1800} composite membrane for 50 mg/L CR aqueous solution.

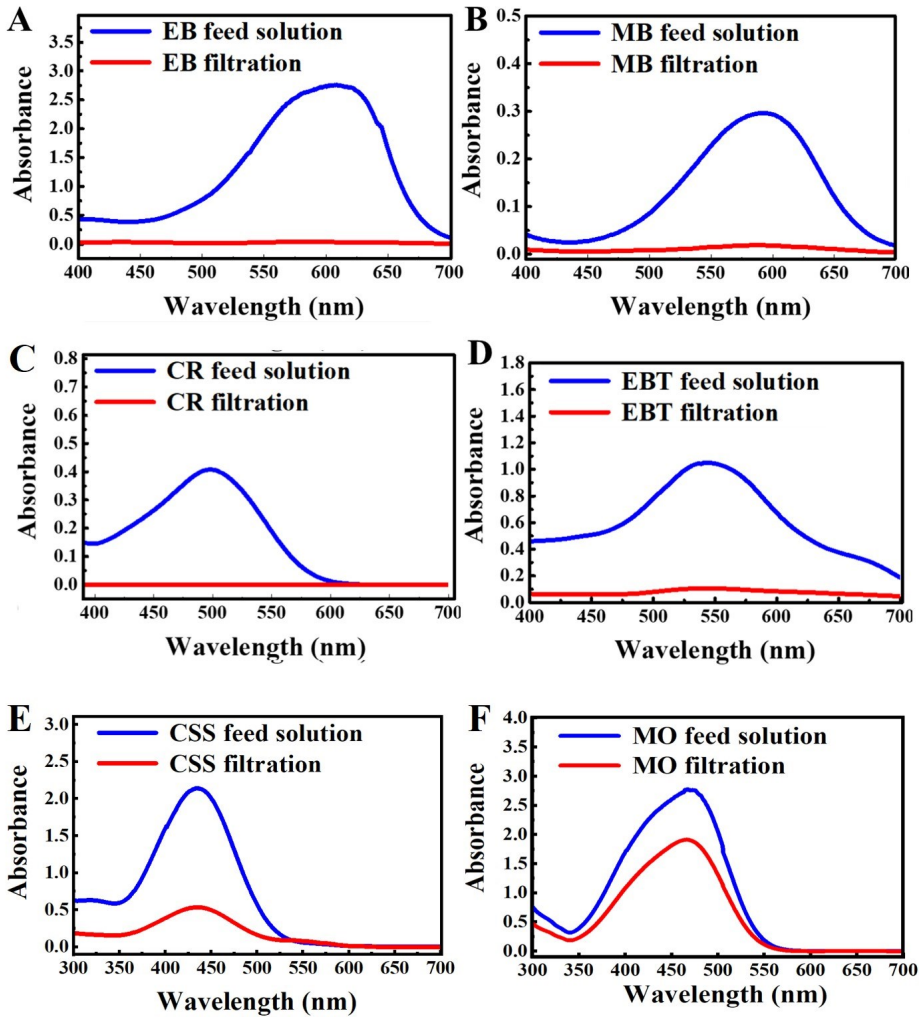

Fig. S19 The rejection efficiency of the GR/GO@PEI_{1800} composite membrane for anionic dye molecule: (A) EB, (B) MB, (C) CR, (D) EBT, (E) CSS, (F) MO solution, respectively.

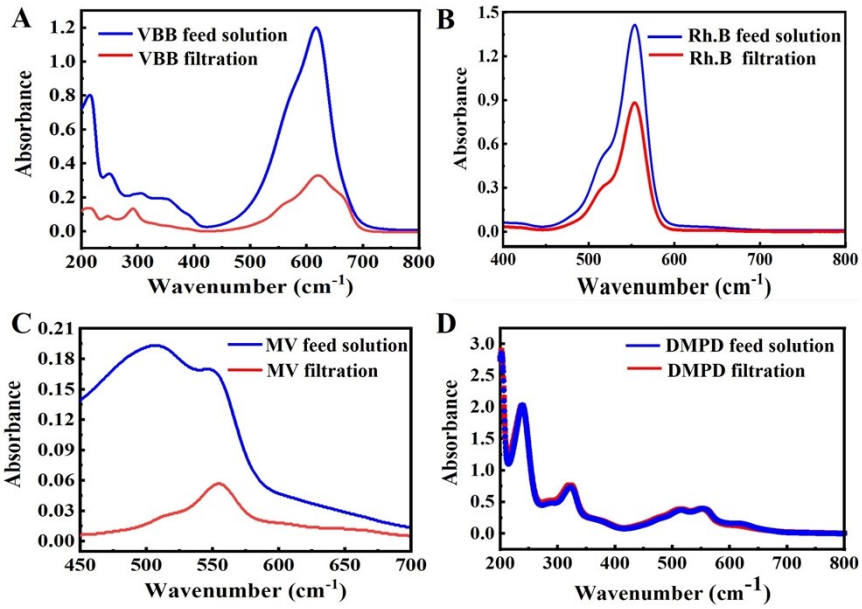

Fig. S20 The rejection efficiency of the GR/GO@PEI_{1800} composite membrane for cationic dye molecule: (A) VBB, (B) Rh. B, (C) MV, (D) DMPD solution, respectively.

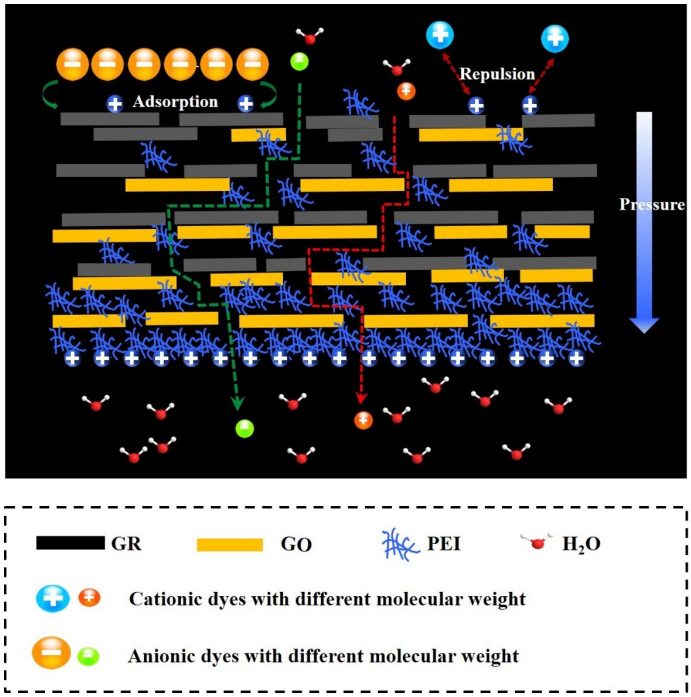

Fig. S21 The separation mechanism of the GR/GO@PEI_{1800} composite membrane for various dyes, which was attributed to the collective effect of size screening and Donnan balance

The separation mechanism of this composite membrane for various dyes was shown in **Fig. S21.** On the one hand, the rejection of the dye molecules was attributed to the collective effect of size screening

(*Adv. Funct. Mater. 2019, 29, 1902014*). The interlayer spacing of the GR/GO@PEI_{1800} composite membrane is the two-dimensional pore size of the separation membrane. According to the size sieving theory, a separation membrane can allow particles smaller than its pore size to permeate through the membrane, while components larger than its pore size are retained. Therefore, the GR/GO@PEI_{1800} composite membrane can be used for the separation of various dye molecules with different molecular weights or sizes. On the other hand, the rejection of the dye molecules was due to Donnan balance (*Science, 2014, 343, 740-742; Sci China Mater 2018, 61, 1021-1026*). As to anionic dye molecules, they were adsorbed on the composite membrane interface due to the electrostatic force. Under this case, the concentration of anion ion in the composite membrane was greater than that in the solution. Whereas, the concentration of the cation ion of cationic dye molecules in the composite membrane was lower than that in the feed. The resulting Donnan position difference can prevent the diffusion of cation ion from the feed into the composite membrane and the anion ion of cationic dye molecules were rejected on the membrane surface in order to maintain electrical neutrality. However, with regard to cationic dyes, they were rejected on the surface of the membrane surface because of the charge repulsion effect. Similarly, the anion ion in the cationic dyes were rejected on the membrane surface in order to keep charge balance. Therefore, the rejection of the dye molecules was attributed to the collective effect of size screening and Donnan balance.

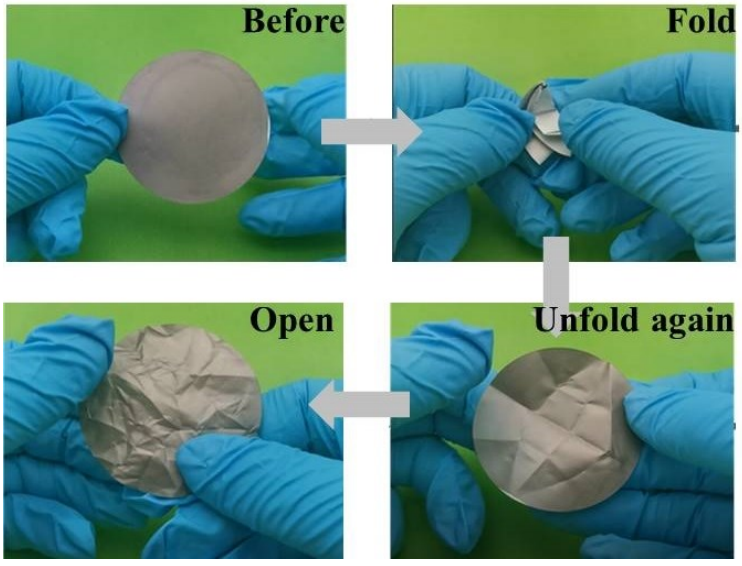

Fig. S22 The GR/GO@PEI_{1800} composite membrane can be bent for several times and maintained its complete structure.

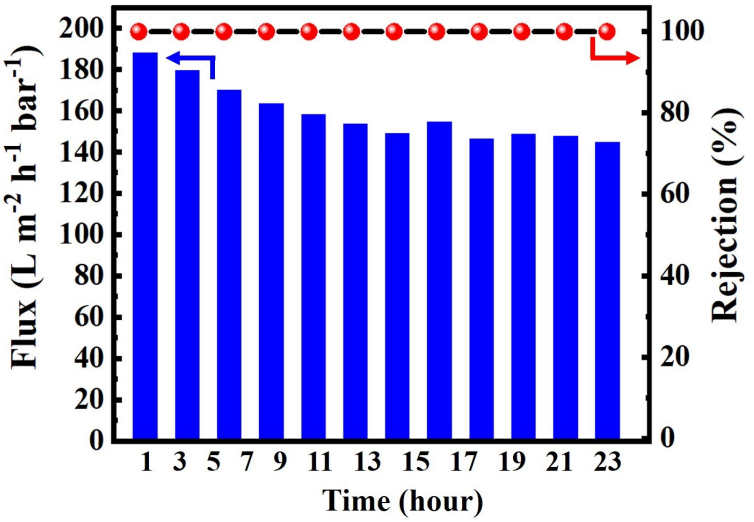

Fig. S23 The separation flux and rejection ability of the GR/GO@PEI composite membrane for CR solution after separation for 23 hours.

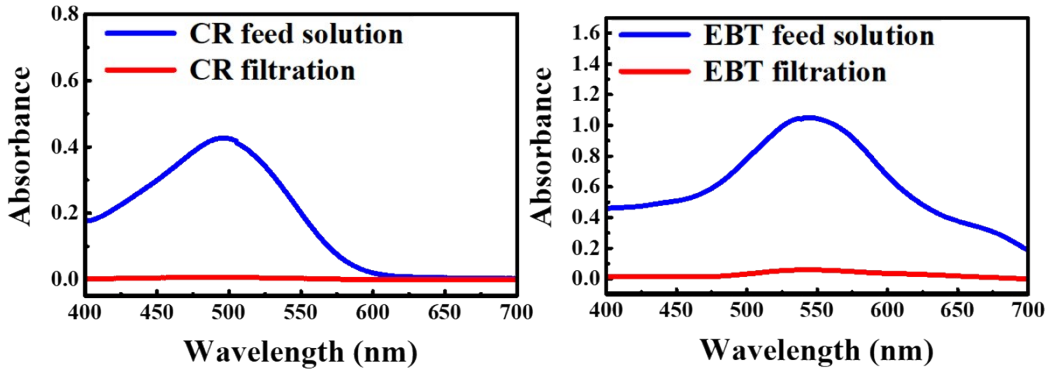

Fig. S24 Rejection efficiency of the GR/GO@PEI_{1800} membrane module for CR and EBT, respectively.

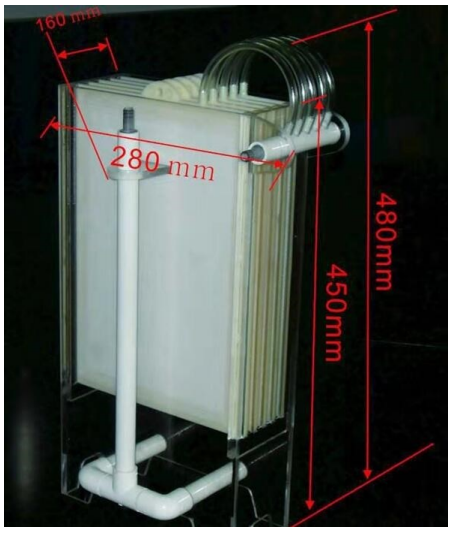

Fig. S25 The purification device with the GR/GO@PEI_{1800} composite membrane as a core.

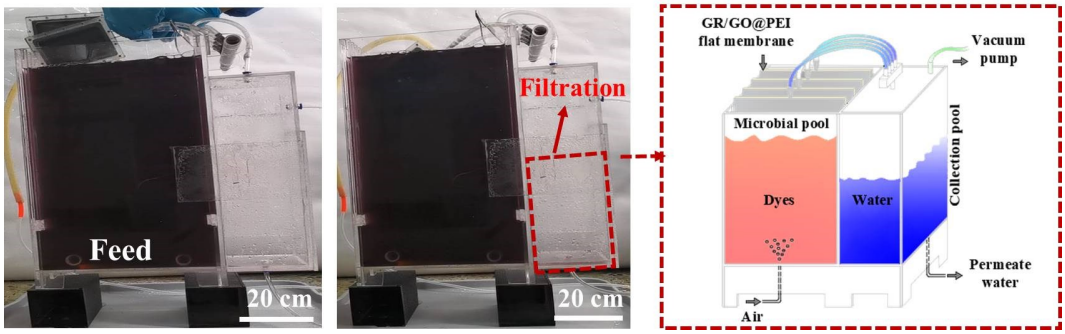

Fig. S26 Photographs of membrane separation purification device with the GR/GO@PEI composite membrane as a core to purify complex multi-component domestic sewage system.

Table S1 The pure water flux of previous reported GO-based membranes in literatures.

Membranes	Preparation methods	Pure water fluxes	Reference
GR/GO@PEI	**Interfacial Self-assembled**	**254 L m^{-2} h^{-1} bar^{-1}**	**This work**
GO/g-PSf	Vacuum-assisted filtration	44 L m^{-2} h^{-1} bar^{-1}	[1]
PEBAX®1657/CS/CNT	Stretch film	6.5 L m^{-2} h^{-1} bar^{-1}	[2]
GO/SiO_2	Vacuum-assisted filtration	5.1 L m^{-2} h^{-1} bar^{-1}	[3]
COF-GO	Vacuum-assisted filtration	31 L m^{-2} h^{-1} bar^{-1}	[4]
POFG/Acryl	Casted	79 L m^{-2} h^{-1} bar^{-1}	[5]
GO/TiO_2	In situ oxidation	89.6 L m^{-2} h^{-1} bar^{-1}	[6]
COF-TpPa/GO	Hot-pressing method	166.8 L m^{-2} h^{-1} bar^{-1}	[7]
GO/PEI-10000	Chemical modification	450.2 L m^{-2} h^{-1} bar^{-1}	[8]
Carbon fibres	Vacuum-assisted filtration	43.4 L m^{-2} h^{-1} bar^{-1}	[9]
GO/PEI/GDL	Vacuum-assisted filtration	274.1 L m^{-2} h^{-1} bar^{-1}	[10]
GO/TEOA	Vacuum-assisted filtration	8 L m^{-2} h^{-1} bar^{-1}	[11]
rGO/PDA	Chemical modification	24 L m^{-2} h^{-1} bar^{-1}	[12]
GO/Fe_3O_4/PES	Vacuum-assisted filtration	58 L m^{-2} h^{-1} bar^{-1}	[13]

GO/IPDI	Chemical modification	84.5 L m^{-2} h^{-1} bar^{-1}	[14]
GO/Epoxy	Physical crosslinking	6.8 L m^{-2} h^{-1} bar^{-1}	[15]
PNIPAM/GO	Chemical modification	12 L m^{-2} h^{-1} bar^{-1}	[16]
GO/PAN	Vacuum-assisted filtration	8 L m^{-2} h^{-1} bar^{-1}	[17]
GO/CS	Vacuum-assisted filtration	10 L m^{-2} h^{-1} bar^{-1}	[18]
Monolayer GR	O_2 Plasma treatment	252 L m^{-2} h^{-1} bar^{-1}	[19]
QA/GO/CS	Solvent induced phase separation	21 L m^{-2} h^{-1} bar^{-1}	[20]

Table S2 The separation fluxes and rejections of the previously reported separation membranes for CR.

Membranes	**Preparation methods**	**Fluxes and rejections**	**Reference**
GR/GO@PEI	**Interfacial Self-assembled**	**191 L m^{-2} h^{-1} bar^{-1} (CR, R=99.8%)**	**This work**
GO/g-PSf	Vacuum-assisted filtration	13.5 L m^{-2} h^{-1} bar^{-1} (CR, R=99.8%)	[1]
MoS_2/GO	Vacuum-assisted filtration	35 L m^{-2} h^{-1} bar^{-1} (CR, R=99.9%)	[21]
NH_2-Fe_3O_4/GO	Vacuum-assisted filtration	14.6 L m^{-2} h^{-1} bar^{-1} (CR, R=98%)	[22]
rGO-TiO_2	Vacuum-assisted filtration	9.5 L m^{-2} h^{-1} bar^{-1} (CR, R=98.7%)	[23]
COF-GO	Vacuum-assisted filtration	28.4 L m^{-2} h^{-1} bar^{-1} (CR, R=99.9%)	[4]
rGO/PDA	Chemical modification	20 L m^{-2} h^{-1} bar^{-1} (CR, R=98.0%)	[12]
GO/IPDI	Chemical modification	95 L m^{-2} h^{-1} bar^{-1} (CR, R=98.2%)	[14]
GO	Chemical modification	190 L m^{-2} h^{-1} bar^{-1} (CR, R=87%)	[24]
GO/PAN	Vacuum-assisted filtration	2.1 L m^{-2} h^{-1} bar^{-1}	[17]

		(CR, R=87%)	
PDDA/GO/PAN	Layer by Layer self-assembly	5.8 L m^{-2} h^{-1} bar^{-1} (CR, R=99.9%)	[25]
PEI-GO/PAA/PVA/GA	Layer by Layer self-assembly	0.84 L m^{-2} h^{-1} bar^{-1} (CR, R=99.5%)	[26]
PPTA/PVDF	Dry-wet spinning method	91 L m^{-2} h^{-1} bar^{-1} (CR, R=99%)	[27]
PIP/TA	TAIP method	32.57 L m^{-2} h^{-1} bar^{-1} (CR, R=99.4%)	[28]
MBFM(40)/PAN	Chemical modification	126 L m^{-2} h^{-1} bar^{-1} (CR, R=99.9%)	[29]
pDA/PEI/Co^{2+}	Chemical modification	104 L m^{-2} h^{-1} bar^{-1} (CR, R=100%)	[30]
PVDF/F-SiO_2	Chemical modification	83.5 L m^{-2} h^{-1} bar^{-1} (CR, R=17.8%)	[31]
PVDF/Ni	Dip-coating	137.5 L m^{-2} h^{-1} bar^{-1} (CR, R=100%)	[32]
phos-(PEI)/HPAN	Cross-linking	5.5 L m^{-2} h^{-1} bar^{-1} (CR, R=99.4%)	[33]
COF-LZU1	Vacuum-assisted filtration	106.86 L m^{-2} h^{-1} bar^{-1} (CR, R=98.6%)	[34]
PEI/PAA	Sacrificial template method	166 L m^{-2} h^{-1} bar^{-1} (CR, R=96.3%)	[35]
PEI/GA/HPAN	Chemical modification	51 L m^{-2} h^{-1} bar^{-1} (CR, R=97.1%)	[36]
CMCNa/PEI/PP	Cross-linked	5.7 L m^{-2} h^{-1} bar^{-1} (CR, R=99.4%)	[37]
CA-MWCNT	Outspread	19.56 L m^{-2} h^{-1} bar^{-1} (CR, R=99.19%)	[38]
PVDF-SAN	Chemical modification	23.75 L m^{-2} h^{-1} bar^{-1} (CR, R=97.7%)	[39]
PAN-g-PEO	Free-radical polymerization	85 L m^{-2} h^{-1} bar^{-1} (CR, R=96%)	[40]
Commercial membrane (PF45)	Phase inversion	5 L m^{-2} h^{-1} bar^{-1} (CR, R=100%)	[41]

Reference

[1] J. Li, M.Y. Hu, H.C. Pei, X. H Ma, F. Y, D. S. Dlamini, Z. Y. Cui, B. Q. He, J. X. Li and H. Matsuyama, *J. Membr. Sci.*, 2020, 595, 117547.

[2] S. R. Mousavi, M. Asghari and N. M. Mahmoodi, *Carbohyd. Polym.*, 2020, 237, 116128.

[3] P. Zhanga, J. L. Gong, G. M. Zeng, B. Song, W. C. Cao, H. Y. Liu, S. Y. Huan and P. Peng, *J. Membr. Sci.*, 2019, 574, 112-123.

[4] X. K. Zhang, H. Li, J. Wang, D. L. Peng, J. D. Liu and Y. T. Zhang, *J. Membr. Sci.*, 2019, 581, 321-330.

[5] J. Balapanuru, K. K Manga, W. Fu, I. Abdelwahab, G. Zhou, M. X. Li, H. B. Li and K. P. Loh, *Desalination*, 2019, 451, 72-80.

[6] R. Y. Han, and P. Y. Wu, *J. Mater. Chem. A*, 2019, 7, 6475-6481.

[7] G. D. Kong, J. Pang, Y. C. Tang, L. L. Fan, H. X. Sun, R. M. Wang, S. Feng, Y. Feng, W. D. Fan, W. P. Kang, H. L. Guo, Z. X. Kang and D. F. Sun, *J. Mater. Chem. A*, 2019, 7, 24301-24310.

[8] J. J. Lu, Y. H. Gu, Y. Chen, X. Yan,Y. J. Guo and W. Z. Lang, *Sep. Purif. Technol.*, 2019, 210, 737-745.

[9] W. Chen, S. Y. Chen, T. F. Liang, Q, Zhang, Z. L. Fan, H. Yin, K. W. Huang, X. X. Zhang, Z. P. Lai and P. Sheng, *Nat. Nanotechnol.*, 2018, 13, 345-350.

[10] K. Changwoo, S. Y. An, J. Lee, Q. Q. Zeng and J. D. Fortner, *ACS Appl. Mater. Interf.*, 2018, 11, 924-929.

[11] K. Nakagawa, S. Araya, M. Kunimatsu, T. Yoshioka, T. Shintani, E. Kamio and H. Matsuyama, *Membranes*, 2018, 8, 130.

[12] J. Ma, Y. He, G. Zeng, F. Li, Y. Li, J. Xiao and S. Yang, *Polym. Adv. Technol.*, 2018, 29, 941-950.

[13] G. Abdi, A. Alizadeh, S. Zinadini and G. Moradi, *J. Membr. Sci.*, 2018, 552, 326-335.

[14] P. Zhang, J. L. Gong, G. M. Zeng, C. H. Deng, H. C. Yang, H. Y. Liu and S. Y. Huan, *Chem. Eng. J.*, 2017, 322, 657-666.

[15] J. Abraham, K. S. Vasu, C. D. Williams, K. Gopinadhan, Y. Su, C.T. Cherian, J. Dix, E. Prestat, S. J. Haigh, I. V. Grigorieva, P, Carbone, A. K. Geim and R. R. Nair, *Nat. Nanotechnol.*, 2017, 12, 546-550.

[16] J. C. Liu, N. Wang, L. J. Yu, A. Karton, W. Li, W. X. Zhang, F. Y. Guo, L. L. Hou, Q. F. Cheng, L and D. A. Weitz, *Nat. Commun.*, 2017, 8, 2011.

[17] J. Wang, P. Zhang, B. Liang, Y. Liu, T. Xu, L. Wang, B. Cao and K. Pan, *ACS Appl. Mater. Interf.*, 2016, 8, 6211-6218.

[18] K. Huang, G. P. Liu, J. Shen, Z. Y. Chu, H. L. Zhou, X. H. Gu, W. Q. Jin and N. P. Xu, *Adv. Funct. Mater.*, 2015, 25, 5809-5815.

[19] S. P. Surwade, S. N. Smirnov, I. V. Vlassiouk, R. R. Unocic, G. M. Veith, S. Dai and S. M. Mahurin, *Nat. Nanotechnol.*, 2015, 10, 459-64.

[20] J. Guo, K. Y. Zhao, X. X. Zhang, Z. J. Cai, M. Chen, T. Chen and J. F. Wei, *Mater. Lett.*, 2015, 157, 112-115.
[21] J. Ma, X. D. Tang, Y. He, Y. Fan, J. Y. Chen and H. Yu, *Desalination*, 2020, 480, 114328.
[22] L. L. Dong, M. H. Li, S. Zhang, X. J Si, Y. X. Bai and C. F. Zhang, Desalination, 2020, 476, 114227.
[23] J. Yu, Y. Zhang, J. H. Chen, L. L. Cui and W. H. Jing, *J. Membr. Sci.*, 2020, 600, 117870.
[24] A. Colomba, B. Mark, R. Divigalpitiya, F. Brandys and J. Gilroy, *Can. J. Chem.*, 2017, 95, 1103-1109.
[25] L. Wang, N. Wang, J. Li, J. Li, W. Bian and S. Ji, *Sep. Purif. Technol.*, 2016, 160, 123-131.
[26] N. X. Wang, S. L. Ji, G. J. Zhang, J. Li and L. Wang, *Chem. Eng. J.*, 2012, 213, 318-329.
[27] W. Y. Shi, X. H. Zeng, H. B. Li, H. X. Zhang, X. H. Qin and R. Zhou, *J. Appl. Polym. Sci.*, 2020, 137, 48569.
[28] Q. Li, Z. P. Liao, X. F. Fang, J. Xie, L. H. Ni, D. P. Wang, J. W. Qi, X. Y. Sun, L. J. Wang and J. S. Li, *Desalination*, 2020, 479, 114343.
[29] Q. Q. Yu, X. D. You, H. Wu, Y. L. Su, R. N. Zhang, Y. N. Liu, C. Yang, J. L. Shen, J. Q. Yuan and Z. Y. Jiang, *J. Mater. Chem. A*, 2020, 8, 4505
[30] Y. Q. Zhang, J. Ma and L. Shao, *J. Mater. Chem. A*, 2020, 8, 5078.
[31] S. H. Zhou, Z. Xiong, F. Liu, H. B. Lin, J. Q. Wang, T. T. Li, Q. Han and Q. L. Fang, *J. Mater. Chem. A*, 2019, 7, 632.
[32] W. M. Yu, Y. Liu, Y. C. Xu, R. J. Li, J. R. Chen, B. Q. Liao, L. G. Shen and H. J. Lin, *J. Membr. Sci.*, 2019, 581, 401-412.
[33] P. Li, Z. Wang, L. B. Yang, S. Zhao, P. Song and B. Khan, *J. Membr. Sci.*, 2018, 555, 56-68.
[34] H. W. Fan, J. H. Gu, H. Meng, A. Knebel and J. Caro, *Angew. Chem. Int. Ed.*, 2018, 57, 4083-4087.
[35] Z. Lin, Q. G. Zhang, Y. Qu, M. M. Chen, F. Soyekwo, C. X. lin, A. M. Zhu and Q. L. Liu, *J. Mater. Chem. A*, 2017, 5, 14819-14827.
[36] S. Zhao and Z. Wang, *J. Membr. Sci.*, 2017, 524, 214-224.
[37] Q. Chen, P. P. Yu, W. Q. Huang, S. C. Liu and C. J. Gao, *J. Membr. Sci.*, 2015, 492, 312-321.
[38] J. Guo, K. Y. Zhao, X. X. Zhang, Z. J. Cai, M. Chen, T. Chen and J. F. Wei, *Mater. Lett.*, 2015, 157, 112-115.
[39] H. P. Srivastava, G. Arthanareeswaran, N. Anantharaman, V. M. Starov, *Desalination*, 2011, 282, 87-94.
[40] A. Asatekin, E. A. Olivetti and A. M. Mayes, *J. Membr. Sci.*, 2009, 332, 6-12.
[41] M. G. Buonomenna, L. C. Lopez, P. Favia, R. d'Agostino, A. Gordano and E. Drioli, *Water res.*, 2007, 41, 4309-4316.